A facile route to synthesize magnetic particles within hollow mesoporous spheres and their performance as separable Hg^{2+} adsorbents

Limin Guo,[a] Jiangtian Li,[a] Lingxia Zhang,[a] Jingbo Li,[a] Yongsheng Li,[b] Chichao Yu,[a] Jianlin Shi,*[a] Meiling Ruan[a] and Jingwei Feng[a]

Received 19th February 2008, Accepted 26th March 2008
First published as an Advance Article on the web 14th April 2008
DOI: 10.1039/b802857e

We present here a simple and effective strategy, called the vacuum nano-casting route (VNR), for fabricating hollow mesoporous spheres with magnetic cores. The loading amount of magnetic cores and saturation magnetization value can be easily tuned by changing the concentration of iron nitrate solution used in the synthesis procedure. After modification with 1,4-bis(triethoxysilyl)propane tetrasulfide (BTESPTS), the composite could be used as a highly selective absorbent of Hg^{2+}, and was conveniently separated by an external magnetic field. The composites are characterized by X-ray diffraction, N_2 sorption isotherms, transmission electron microscopy, energy-dispersive spectroscopy, vibrating-sample magnetometry, Fourier-transform infrared spectroscopy and inductively coupled plasma atomic emission spectroscopy.

Introduction

Ordered mesoporous materials have attracted considerable attention since they were first reported for potential applications in heterogeneous catalysis, host–guest chemistry, environmental technology, adsorption, chemical sensing, electrochemistry and drug delivery because of their large specific surface area, large pore volume, uniform pore size distribution, and easily modified pore surface.[1,2] Hollow mesoporous spheres with mesoporous shells exhibit more advantages in mass diffusion and transportation compared with conventional mesoporous materials due to their larger pore and cavity volumes and spherical morphology.[3,4] A number of reports have described the formation of hollow mesoporous silica spheres (HMS) in the past few years.[3–10] In general, there are two ways for the synthesis of hollow mesoporous spheres. One is *via* a "soft-template" route, such as using poly(vinylpyrrolidone) (PVP) and cetyltrimethylammonium bromide (CTAB),[3] tetrapropylammonium hydroxide (TPAOH) and CTAB,[4] and just CTAB[6] as the template for HMS; the other is *via* a "hard-template" route, such as using polystyrene spheres and CTAB as co-templates for HMS,[5,8] hard silica core/mesoporous silica shell as the template for hollow mesoporous carbon spheres[7] or HMS.[10] Our group has synthesized one kind of hollow mesoporous aluminosilicate spheres (HMAS) with a three-dimensional pore network and high hydrothermal stability.[4] The mesopore channels can retain their cubic order after treatment in a pure-water stream for 60 h or in boiling water for 120 h. Hollow spheres have more advantages in mass diffusion, chemical catalysis and can stand harsh surface modification for practical applications. On the other hand, magnetic particles embedded in mesoporous materials have been intensively pursued for emerging applications in targeted drug delivery and efficient separable catalysis or adsorption.[11] Thanks to their mesoporous structure, spherical morphology and magnetism, mesoporous spheres incorporated with magnetic particles have attracted great attention. There have been some reports on the preparation of magnetic particles coated with mesoporous shells.[12–15] The magnetic core/mesoporous silica shell structures were synthesized by coating mesoporous silica shells on hematite particles through sol–gel reactions followed by H_2 reduction.[12] Magnetic nanocrystals[13] or GdSe/ZnS quantum dots[14] could also be directly embedded in mesoporous silica spheres by sol–gel reactions. In these reports, hematite particles and magnetic nanocrystals were firstly synthesized, and then were coated with a mesoporous silica shell. It can be seen that these synthesis procedures required very strict control over the synthesis conditions and the yields were relatively low. Very recently, Fuertes and co-workers[15] reported an incipient wetness impregnation technique to synthesize carbon capsules with a variety of inorganic materials. This method is attractive, however the inorganic solution has to be added dropwise until incipient wetness, and the procedure should be repeated several times for the desired loading amount, so the synthesis is very time-consuming and the yield is low, too. Herein, we report a new and very facile route to fabricate hollow mesoporous aluminosilicate spheres with magnetic cores (HMASMCs). In this synthesis procedure, HMAS was mixed with a solution of Fe source, and the system was then placed under vacuum, so the Fe source could be introduced into the hollow cores of HMAS as driven by the environmental air pressure.

Removal of toxic heavy metal ions from wastewater is a continuing research objective of environmental pollution control.[16] Various materials, such as ion exchange resins, activated charcoal and ion chelating agents immobilized on

[a]*State Key Lab of High Performance Ceramics and Superfine Microstructure, Shanghai Institute of Ceramics, Chinese Academy of Science, 1295 Dingxi Road, Shanghai, 200050, P. R. China. E-mail: jlshi@sunm.shcnc.ac.cn*
[b]*School of Materials Science and Engineering, East China University of Science and Technology, 130 Meilong Road, Shanghai, 200237, P. R. China*

inorganic supports, have been used as heavy metal absorbents.[17] However, these materials exhibits many drawbacks because of their wide distribution of pore sizes, heterogeneous pore structure, low selectivity and low loading capacities for heavy metal ions. Considerable efforts have been devoted to the preparation of mesoporous silica-based absorbents due to their unique large surface area, well-defined pore size and shape and well-modified surface properties.[16a,b,18–25] The materials for this application generally need to exhibit specific sites with affinity for heavy metal ions, but most mesoporous materials themselves do not have such surface properties.[16a] Accordingly, the methods of post-grafting and co-condensation were developed so that functional chemical groups can be bonded to the pore surfaces of silica-base mesoporous materials. Many chemical molecules containing useful functional groups, such as thiol,[16a,20,22] thioether,[16b] and amino[24,25] groups, have been used to modify the surface of silica-base mesoporous materials. These functionalized hybrid materials show good adsorption capacity and selectivity for metal ions. If these functionalized hybrid materials exhibited magnetic properties, the composite adsorbents would be easily separated from the aqueous systems by an external magnetic field. In this way, lower operation costs in absorbent separation and recycling procedures for wastewater treatment could be achieved. Herein, we functionalized HMASMCs with thioether by the post-grafting method, and the composite structure exhibits highly selective adsorption for Hg^{2+} and easy magnetic separation.

Experimental

Materials preparation

Materials: Tetrapropylammonium hydroxide (TPAOH, 20% in water) was from Aldrich. Cetyltrimethylammonium bromide (CTAB, 99%), tetraethyl orthosilicate (TEOS, 98%), sodium hydroxide, aluminium sulfate ($Al_2(SO_4)_3 \cdot 18H_2O$), iron nitrate ($Fe(NO_3)_3 \cdot 9H_2O$), mercuric nitrate ($Hg(NO_3)_2 \cdot 0.5H_2O$), cupric nitrate ($Cu(NO_3)_2 \cdot 3H_2O$), cadmium nitrate ($Cd(NO_3)_2 \cdot 4H_2O$), lead nitrate ($Pb(NO_3)_2$), zinc nitrate ($Zn(NO_3)_2 \cdot 6H_2O$), hydrogen chloride (36–38%) and absolute ethyl alcohol were purchased from Sinopharm Chemical Reagent Co. and used without further purification. Molecular sieves type 4A was purchased from Sinopharm Chemical Reagent Co. and was dewatered by calcination at 673 K for 2 h before use. Toluene was purchased from Shanghai Lingfeng Chem. Co. and was dewatered by molecular sieves for 24 h before use. 1,4-Bis(triethoxysilyl)propane tetrasulfide (BTESPTS) was purchased from Nanjing Shuguang Chem. Co. and used without further purification.

Hollow mesoporous aluminosilicate spheres (HMAS) were synthesized by our method described previously.[4]

Preparation of hollow mesoporous aluminosilicate spheres with magnetic cores (HMASMC): A certain amount of HMAS was added to an ethanol solution of iron nitrate (0.25 M and 1.0 M concentrations were used in the synthesis procedure), and the turbid suspension was subjected to vacuum under ultrasonic conditions (SK3300HP 59 kHz, 160 W). After thirty minutes, the vacuum pump was turned off and air was allowed to enter the system till normal atmospheric pressure was achieved, while the ultrasonic treatment continued, and the system status was held for ten minutes. After that, the iron nitrate solution was removed by centrifugation and the precipitate was dried under flowing air at room temperature. After drying, the powder was washed twice with absolute ethanol. Then, the powder was dried under flowing air again. After that, the powder was calcined at 773 K for 2 h to yield the hollow mesoporous aluminosilicate spheres with hematite cores (HMASHCs). The reduction was carried out by the thermal treatment of the HMASHC particles in mixed H_2 (5% volume percentage) and Ar (95% volume percentage) gases at 683 K for 3 h, and the final HMASMCs were obtained.

HMAS was also immersed in 1.0 M iron nitrate solution under normal atmosphere for 24 h, instead of the vacuum nano-casting route, to provide a reference for comparison, named C-HMAS.

Preparation of HMASMC modified by BTESPTS: 1.0g 1.0 M HMASMC, 80 mL dewatered toluene and 20 mL BTESPTS were added into a flask, and refluxed under N_2 atmosphere for 48 h. After that, the modified HMASMCs were separated and then dried in a vacuum oven for 24 h at room temperature.

Hg^{2+} selective adsorption and separation experiments: For the preparation of aqueous metal solutions, the following metal nitrates were used: $Hg(NO_3)_2 \cdot 0.5H_2O$, $Cu(NO_3)_2 \cdot 3H_2O$, $Cd(NO_3)_2 \cdot 4H_2O$, $Pb(NO_3)_2$, $Zn(NO_3)_2 \cdot 6H_2O$; see Table 2 (later) for their concentrations. Hydrochloric acid was used to prevent the precipitation of the metal ions during the adsorption experiment (for 1 L metal ion solution, 5 mL 2M HCl was added). 0.5 g modified HMASMCs was added into 30 mL wastewater and stirred for 24 h. Then, one half of the suspension was separated by an external magnetic field and the other half by centrifugation for comparison.

Regeneration of mercury-loaded absorbents: The mercury-loaded absorbents were rapidly washed with concentrated HCl (12.1 M), then separated by an external magnetic field, and then washed three times with de-ionized water. After that, the absorbents were dried in a vacuum oven at 323K. The dried absorbents after first and second regenerations were designated as B-HMASMC-1R and B-HMASMC-2R, respectively.

Characterization: Powder XRD patterns were recorded on a Rigaku D/Max-2550V diffractometer using Cu Kα radiation (40 kV and 40 mA). The scanning rate was 0.6 and 6° min^{-1} for low-angle and high-angle measurements, respectively. Nitrogen sorption isotherms at 77 K were measured on a Micrometitics Tristar 3000 system. Before measurement, samples were pre-treated at 373 K for 12 h under nitrogen. The specific surface area and the pore size distribution were calculated from the BET and Barrett–Joyner–Halenda (BJH) data, respectively. TEM images were obtained on a JEM-2010 electron microscope operated at 200 kV. EDX spectra were collected from an attached Oxford Link ISIS energy-dispersive spectrometer fixed on the JEM-2010 electron microscope. A vibrating-sample magnetometer (PPMS Model 6000 Quantum Design, San Diego, USA) was used to study the magnetic properties. FTIR spectra were obtained in the range of 400–4000 cm^{-1} using a Nicolet 7000-C with a resolution of 8 cm^{-1}; the powders were dispersed in KBr pellets. The ion concentrations of original and after-adsorbed wastewaters were obtained by inductively coupled plasma atomic emission spectroscopy (ICP-AES; Varian Co., USA).

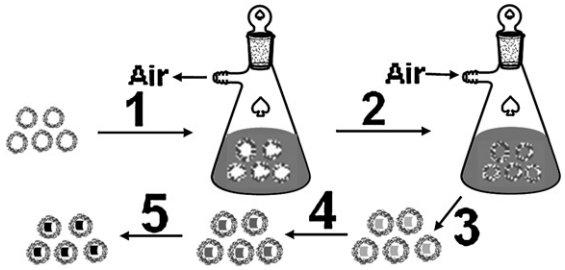

Scheme 1 Schematic illustration of the synthesis procedure of HMASMC composites: (1) addition of HMAS into iron nitrate solution and application of vacuum; (2) pump is switched off and air is allowed to enter; (3) sample separation from the suspension; (4) calcination; (5) reduction.

Results and discussion

Structural studies

Scheme 1 illustrates the schematic procedure, termed the vacuum nano-casting route (VNR), for the synthesis of HMASMCs in the present work. In step 1, as-prepared HMAS was added into the iron nitrate ethanol solution. The environmental pressure in the container was reduced by a vacuum pump, so the air in the hollow part of HMAS could be pumped out. In step 2, the air pressure in the container was adjusted to normal atmosphere; therefore the hollow parts of the HMAS under transitory vacuum conditions would be filled by iron nitrate solution driven by the atmospheric pressure. During steps 1 and 2, ultrasonic treatment was conducted in order to facilitate the removal of air from the hollow cores and the filling of the iron nitrate solution into the hollow parts. In step 3, HMAS containing iron nitrate solution was separated from the suspension. Then, the materials were dried under flowing air at room temperature, and washed twice with absolute ethanol to remove iron nitrate outside of HMAS. In step 4, HMAS with iron nitrate in the hollow cores was calcined in order to obtain iron oxide (hematite) loaded HMAS within cores (HMASHCs). In step 5, the hematite cores within HMAS were reduced into magnetic cores.

Fig. 1 shows the TEM images of (a) as-prepared HMAS, (b) C-HMAS,[26] (c) 0.25M-HMASHC (in the sample synthesis procedure, 0.25 M iron nitrate solution was used), and (d) 1.0M-HMASHC (1.0 M iron nitrate solution was used). Here, C-HMAS (Fig. 1b) has hollow cores like the as-prepared HMAS (Fig. 1a). The images of 0.25M- (Fig. 1c) and 1.0M-HMASHC (Fig. 1d) show that the hematite is loaded into the hollow cores of HMAS, and the loading amount of hematite increases with the increase of the iron nitrate concentration used in the synthesis, indicating that the loading amount of hematite can be easily tuned by changing the concentration of iron nitrate solution.

Fig. 2 shows the low-angle and high-angle X-ray diffraction (XRD) patterns of as-prepared HMAS, C-HMAS, 0.25M- and 1.0M-HMASHC. The as-prepared HMAS and C-HMAS have several diffraction peaks at low angles (Fig. 2a), and these peaks are typical for MCM-48.[4] No diffraction peaks were observed in the high-angle region (Fig. 2b), which indicates the absence of crystalline phases in the samples. For 0.25M- and 1.0 HMASHC, there is one diffraction peak observed at low angle (Fig. 2a), which indicates the two samples still have ordered, though

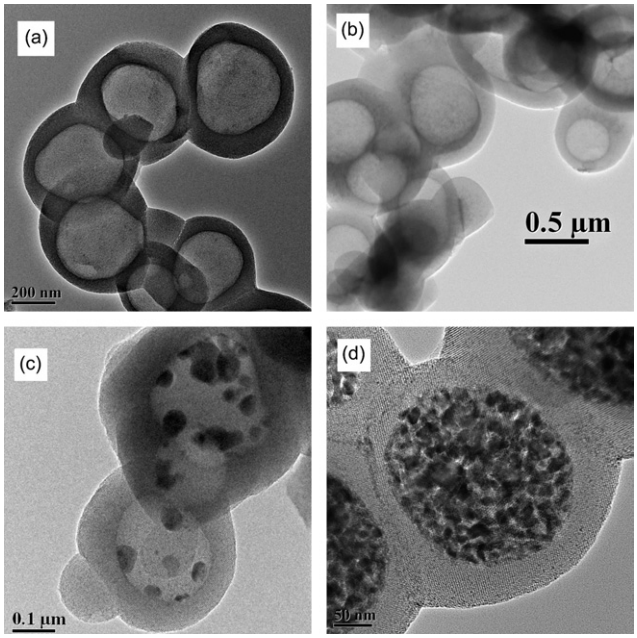

Fig. 1 TEM images of samples (a) HMAS, (b) C-HMAS, (c) 0.25M-HMASHC and (d) 1.0M-HMASHC.

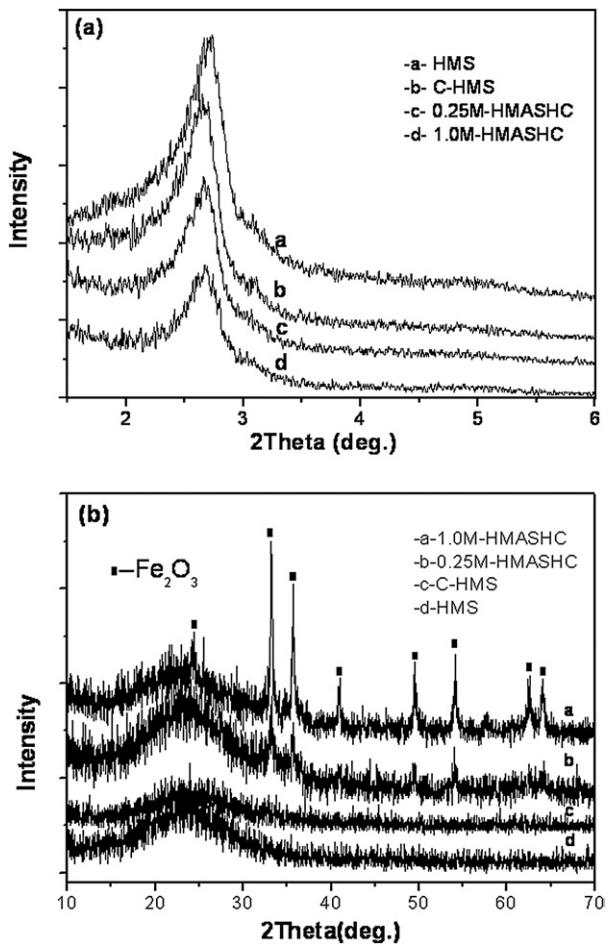

Fig. 2 (a) Low-angle and (b) high-angle XRD patterns of HMAS, C-HMAS, 0.25 HMASHC and 1.0 HMASHC.

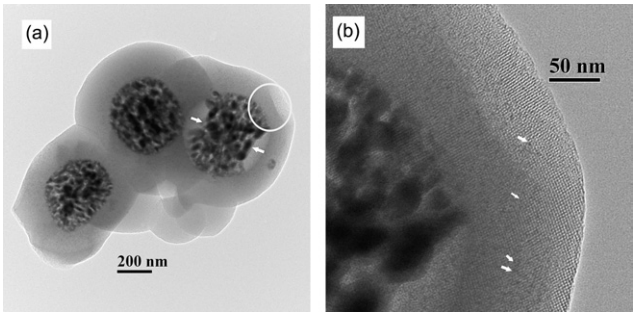

Fig. 3 TEM images of 1.0M-HMASMC.

deteriorated, mesoporous structure. In the high-angle XRD patterns, 0.25M- and 1.0M-HMASHC have several diffraction peaks, and all the peaks match well with the standard PDF data (JCPDS NOS. 33-0664) of hematite, confirming the formation of α-Fe_2O_3. The peak intensity increases following the increase of the iron nitrate concentration used in the synthesis of HMASHC, which indicates the increased loading amount of hematite at higher iron nitrate concentration, in accordance with the results of TEM images (Fig. 1c and d). The above results of TEM observation and XRD patterns prove our hypothesis that the iron nitrate solution could be cast into the hollow cores of HMAS by air pressure.

Fig. 3 is the TEM images of 1.0M-HMASMC. It can be seen that the magnetic cores have shrunk while the shell remains intact (Fig. 3a). A magnified HRTEM image (Fig. 3b) from the circled zone in Fig. 3a shows that the shell has ordered mesopores, and some very small particles (black spots, arrowed) could be found in the HMASMC shell. We think these particles are magnetic particles, and the formation process should be similar to that of those within the cores. In the high-angle XRD patterns of 0.25M- and 1.0M-HMASMC (Fig. 4), several diffraction peaks can be found and all the peaks match well with the standard PDF data (JCPDS nos. 19-0629 and 65-4899), which confirms that the reduced particles in the cores are magnetite and iron. The nanomagnet size was estimated by using the Scherrer equation on the (311) peak of the XRD pattern (Fig. 4), and the iron oxide

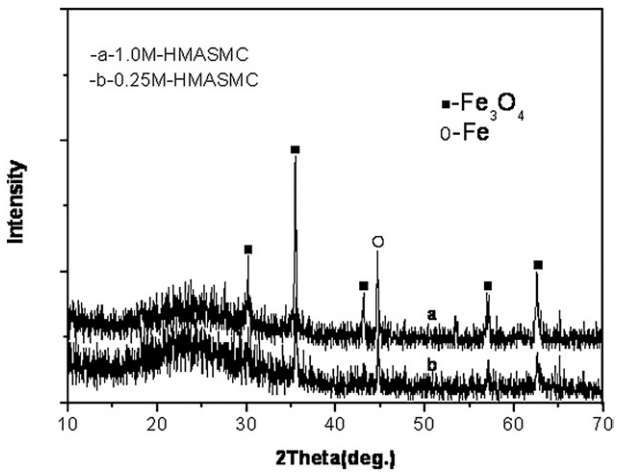

Fig. 4 High-angle XRD patterns of 0.25M-HMASMC (magnetite size 25.3 nm) and 1.0M-HMASMC (magnetite size 43.0 nm).

nanoparticles are calculated to be 25.3 nm for 0.25M-HMASMC and 43.0 nm for 1.0M-HMASMC, approximately in accordance with the TEM image (Fig. 3(b)). The reduction products can be controlled, according to the typical reduction process of hematite: α-$Fe_2O_3 \rightarrow Fe_3O_4 \rightarrow FeO \rightarrow Fe$, by altering the reduction temperature or time.[27] Here, the diffraction intensities of samples increase in accordance with the increase of the loading amount of hematite cores (Fig. 1c,d and Fig. 2b). The magnetization curves of the 0.25M- and 1.0M-HMASMC (Fig. 5a) at room temperature show a magnetic hysteresis loop, which demonstrates the strong magnetic response to a varying magnetic field. The saturation magnetization values of 0.25M- and 1.0M-HMASMC are 3.1 emu g^{-1} and 11.7 g^{-1}, respectively. The coercivity values are 130 Oe for 0.25M-HMASMC and 190 Oe for 1.0M-HMASM, respectively, as estimated from the inset of Fig. 5(a). If the nanomagnet size could be controlled and reduced below the superparamagnetic limit, the magnetic hollow spheres would be more useful and attractive. To attain superparamagnetic properties, one of the effective ways is to develop different synthesis methods which do not need high temperatures for calcination and reduction. The separability of 1.0M-HMASMC was tested in ethanol by placing a magnet beside the glass bottle. Without an outer magnet, the magnetic particles can be dispersed in ethanol to form a stable suspension with black color (inset in Fig. 5b). However, the black particles were attracted to the magnet within several minutes under an external magnetic field (Fig. 5b). According to the above results, the

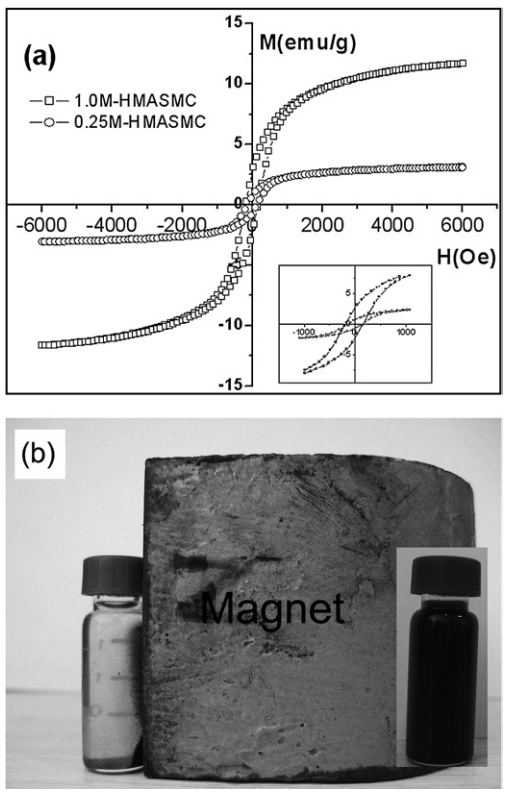

Fig. 5 Magnetic properties of HMASMC at room temperature: (a) magnetization curve, and (b) separation of 1.0M-HMSMC composite particles from suspension under an external magnetic field (inset is the same bottle of sample without the magnetic field).

loading amount of magnetic cores and saturation magnetization values of HMASMC can be easily controlled by altering the iron nitrate concentration during the VNR process.

The N_2 adsorption–desorption isotherms for as-prepared HMAS, C-HMAS, 0.25M- and 1.0M-HMASMC are shown in Fig. 6a. All isotherms show the characteristic of mesoporous materials: type IV isotherms with a marked leap in the adsorption branch at relative pressures P/P_0 between 0.2 and 0.4. This indicates that the ordered mesostructure of HMAS has been kept after loading the magnetic cores. The structure parameters of all samples are summarized in Table 1. Here, similar pore size distributions for all samples, in the range of 2–3 nm, can be found in Fig. 6b and Table 1. The surface area and pore volume of the reference sample C-HMAS are smaller than those of HMAS, due to the iron nitrate solution filling the mesopore channels by capillary force and therefore blocked by formed iron-containing oxide particles. Similarly, the surface area is found to decrease gradually from HMAS, 0.25M-HMASMC to 1.0M-HMASMC, and the pore volume also decreases in the same order. The main reason for such decreases can be attributed to the presence of magnetic cores, which have higher density than silica, and some iron-containing particles in the meso-channels. The blocking of the mesopore channels by iron-containing particles can be found in the TEM images in Fig. 1b and 3b for C-HMAS and 1.0M-HMASMC.

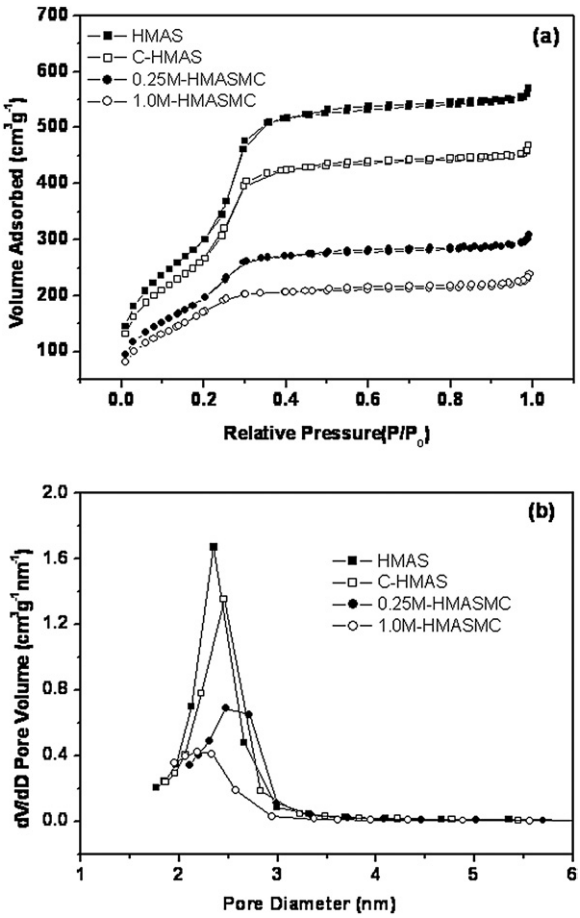

Fig. 6 (a) N_2 adsorption–desorption isotherms and (b) corresponding pore diameter distribution curves of different samples.

Table 1 Structure parameters of samples HMAS, C–HMAS, 0.25M-HMASMC and 1.0M-HMASMC

	S_{BET}[a]/m² g⁻¹	V_{BJH}[b]/cm³ g⁻¹	D_{BJH}[c]/nm
HMAS	1115	0.86	2.35
C-HMAS	985	0.70	2.45
0.25M-HMASMC	732	0.45	2.47
1.0M-HMASMC	648	0.34	2.18

[a] The surface area was calculated according to the BET equation. [b] The pore volume was calculated according to the BJH method at $P/P_0 = 0.97$. [c] The pore diameter was calculated according to the BJH method from N_2 adsorption isotherms.

According to the above analysis, HMASMC can be synthesized by VNR, and the loading amount of magnetic cores and saturation magnetization values can be easily tuned by changing the concentration of iron nitrate solution. Although the surface area and pore volume of HMASMC have decreased compared to as-prepared HMAS, they are still as high as 648 $m^2\ g^{-1}$ and 0.34 $cm^3\ g^{-1}$, respectively, for 1.0M-HMASMC.

Metal ion selective adsorption and separation

The Fourier-transform infrared (FTIR) spectra of as-synthesized 1.0M-HMASMC and BTESPTS modified 1.0M-HMASMC (B-HMASMC) are shown in Fig. 7. The intensity of the absorption peak of the Si–OH (960 cm^{-1}) bond decreases apparently from as-synthesized 1.0M-HMASMC to modified 1.0M-HMASMC, and the adsorption peaks of C–H (2900–3000 cm^{-1}), C–C, C–H_2 (1300–1500 cm^{-1}), and S–S, S–C (520–720cm^{-1}) appear,[28] indicating that BTESPTS has been grafted on the surface of HMASMC.

The concentrations of metal contaminants in wastewater solutions before and after treatment with modified 1.0M-HMASMC are shown in Table 2. It can be seen that the mercury concentration was remarkably reduced, while concentrations of other metal ions show little decrease. This means that thioether functionalized HMASMC exhibits a much higher complexation affinity for Hg^{2+} as compared with the other metal ions. The

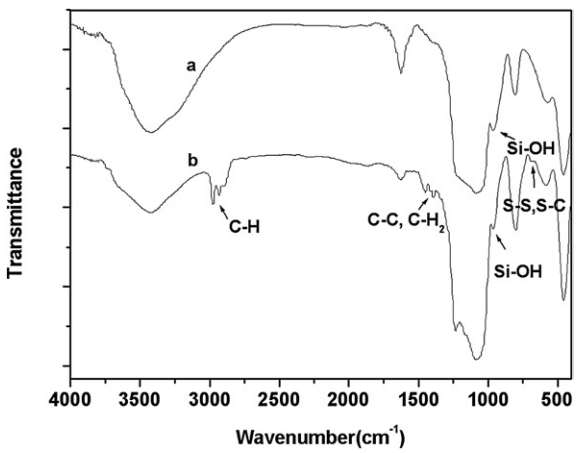

Fig. 7 FTIR spectra of a) as-synthesized 1.0M-HMASMC; and b) 1.0M-HMSAMC modified with BTESPTS.

Table 2 Concentrations of metal ions in simulated wastewater solutions before and after adsorption

	Hg^{2+} (ppm)	Pb^{2+} (ppm)	Cd^{2+} (ppm)	Zn^{2+} (ppm)	Cu^{2+} (ppm)
Original solution	93.8	104.0	196.0	132.4	113.8
C-B-HMASMC[a]	0.6	103.2	194.8	131.0	110.4
M-B-HMASMC[b]	1.0	103.8	195.2	131.7	111.6
M-B-HMASMC-1R	3.9	103.6	196.8	128.4	113.6
M-B-HMASMC-2R	7.6	103.2	195.8	130.6	114.2

[a] C-B-HMASMC was separated by centrifugation. [b] M-B-HMASMC was separated by an external magnetic field.

magnetic separation of B-HMASMC after adsorption is also demonstrated and the results are totally the same as before adsorption as shown in Fig. 5. The composite particles after adsorption can be attracted towards a magnet within a short time period (usually within several minutes), and the composite particles can be re-suspended in the solution once the magnetic field is removed. No apparent differences of the ion concentrations in treated wastewater can be found between different separation methods (centrifugation or external magnetic field) of the absorbents from the suspensions. The Hg^{2+} loaded absorbent was regenerated and reused twice. The Hg^{2+} concentrations after adsorption for the first and second recycles were 3.9 ppm and 7.6 ppm, respectively (Table 2). Although the Hg^{2+} concentration after adsorption became slightly higher along with the recycle times, the composite still maintained high selectivity and capacity for Hg^{2+}.

Conclusions

We have successfully fabricated a kind of hollow mesoporous aluminosilicate spheres with magnetic cores (HMASMC) by a new and facile vacuum nano-casting route (VNR). The loading amount of the magnetic cores and saturation magnetization values of HMASMC can be simply tuned by changing the concentration of iron nitrate solution used in the synthesis. Relatively high surface area (648 $m^2\ g^{-1}$), large pore volume (0.34 $cm^3\ g^{-1}$), and ordered mesoporous shells can be obtained for HMASMC which has a magnetization value of 11.7 emu g^{-1}. This facile route can be used to synthesize other kinds of transitional metal oxide core/nanoporous shell structures. When HMASMC was modified by 1,4-bis(triethoxysilyl)propane tetrasulfide (BTESPTS), the composite showed highly selective adsorption for Hg^{2+} and can be easily separated by an external magnetic field. Thus the material is a promising candidate for magnetically separable heavy metal ion adsorbents.

Acknowledgements

The authors gratefully acknowledge the support of this research by the National Science Foundation of China (Grant No. 20571081 and No. 50702072), Chinese Academy of Science (Grant No. KJCX2.YW.M02) and Shanghai Nano-Science Program (Grant No. 05nm05030 and No. 0652nm014).

References

1 (*a*) C. T. Kresge, M. E. Leonowicz, W. J. Roth, J. C. Vartuli and J. S. Beck, *Nature*, 1992, **359**, 710; (*b*) A. Corma, *Chem. Rev.*, 1997, **97**, 2373; (*c*) D. Zhao, J. Feng, Q. Huo, N. Melosh and G. D. Stucky, *Science*, 1998, **279**, 548; (*d*) M. E. Davis, *Nature*, 2002, **417**, 813; (*e*) Y. Wan and D. Zhao, *Chem. Rev.*, 2007, **107**, 2821.
2 (*a*) Y. Zhu, J. Shi, W. Shen, X. Dong, J. Feng, M. Ruan and Y. Li, *Angew. Chem., Int. Ed.*, 2005, **44**, 5083; (*b*) I. Slowing, B. Trewyn, S. Giri and V. Lin, *Adv. Funct. Mater.*, 2007, **17**, 1225; (*c*) M. Vallet-Regí, F. Balas and D. Acros, *Angew. Chem., Int. Ed.*, 2007, **47**, 7548.
3 Y. Zhu, J. Shi, H. Chen, W. Shen and X. Dong, *Microporous Mesoporous Mater.*, 2005, **84**, 218.
4 Y. Li, J. Shi, Z. Hua, H. Chen, M. Ruan and D. Yan, *Nano Lett.*, 2003, **3**, 609.
5 G. Zhu, S. Qiu, O. Terasaki and Y. Wei, *J. Am. Chem. Soc.*, 2001, **123**, 7723.
6 C. Fowler, D. Khushalani and S. Mann, *Chem. Commun.*, 2001, 2028.
7 S. Yoon, K. Sohn, J. Kim, C. Shin, J. Yu and T. Hyeon, *Adv. Mater.*, 2002, **14**, 19.
8 B. Tan and S. Rankin, *Langmuir*, 2005, **21**, 8180.
9 H. Djojoputro, X. Zhou, S. Qiao, L. Wang, C. Yu and G. Lu, *J. Am. Chem. Soc.*, 2006, **128**, 6320.
10 F. Suárez, M. Sevilla, S. Álvarez, T. Valdés-Solís and A. Fuertes, *Chem. Mater.*, 2007, **19**, 3096.
11 (*a*) A. Lu, W. Li, A. Kiefer, W. Schmidt, E. Bill, G. Fink and F. Schüth, *J. Am. Chem. Soc.*, 2004, **126**, 8616; (*b*) S. Giri, B. Trewyn, M. Stellmaker and V. Lin, *Angew. Chem., Int. Ed.*, 2005, **44**, 5038; (*c*) A. Fuertes and P. Tartaj, *Chem. Mater.*, 2006, **18**, 1675; (*d*) A. Fuertes and P. Tartaj, *Small*, 2007, **3**, 275; (*e*) X. Dong, H. Chen, W. Zhao, X. Li and J. Shi, *Chem. Mater.*, 2007, **19**, 3484; (*f*) N. Andersson, R. Corkery and P. Alberius, *J. Mater. Chem.*, 2007, **17**, 2700; (*g*) E. Ruiz-Hernández, A. López-Noriega, D. Arcos, I. Izquierdo-barba, O. Terasaki and M. Vallet-Regí, *Chem. Mater.*, 2007, **19**, 3455.
12 (*a*) W. Zhao, J. Gu, L. Zhang, H. Chen and J. Shi, *J. Am. Chem. Soc.*, 2005, **127**, 8916; (*b*) D. Yi, S. Lee, G. Papaefthymiou and J. Ying, *Chem. Mater.*, 2006, **18**, 614.
13 Y. Deng, D. Qi, C. Deng, X. Zhang and D. Zhao, *J. Am. Chem. Soc.*, 2008, **130**, 28.
14 J. Kim, J. Lee, J. Lee, J. Yu, B. Kim, K. An, Y. Hwang, C. Shin, J. Park, J. Kim and T. Hyeon, *J. Am. Chem. Soc.*, 2006, **128**, 688.
15 A. Fuertes, M. Sevilla, T. Valdes-Solis and P. Tartaj, *Chem. Mater.*, 2007, **19**, 5418.
16 (*a*) A. Liu, K. Hidajat, S. Kawi and D. Zhao, *Chem. Commun.*, 2000, 1145; (*b*) L. Zhang, W. Zhang, J. Shi, Z. Hua, Y. Li and J. Na, *Chem. Commun.*, 2003, 210; (*c*) S. Shin and J. Jang, *Chem. Commun.*, 2007, 4230.
17 Y. Zolotov, O. Petrukhin and G. Malofeeva, *Anal. Chim. Acta*, 1983, **148**, 135.
18 A. Vinu, M. Miyahara, K. Hossain, M. Takahashi, V. Balasubramanian, T. Mori and K. Ariga, *J. Nanosci. Nanotechnol.*, 2007, **7**, 828.
19 (*a*) K. Northcott, H. Kokusen, Y. Komatsu and G. Stevens, *Sep. Sci. Technol.*, 2006, **41**, 1829; (*b*) S. Oshima, J. Perera, K. Northcott, H. Kokusen, G. Stevens and Y. Komatsu, *Sep. Sci. Technol.*, 2006, **41**, 1635.
20 D. Perez-Quintanilla, I. Del Hierro, M. Fajardo and I. Sierra, *J. Mater. Chem.*, 2006, **16**, 1757.
21 H. Yoshitake, *New J. Chem.*, 2005, **29**, 1107.
22 A. Walcarius and C. Delacte, *Anal. Chim. Acta*, 2005, **547**, 3.
23 X. Wu, H. Ma, J. Li, J. Zhang and Z. Li, *J. Colloid Interface Sci.*, 2007, **315**, 555.
24 S. Oh, T. Kang, H. Kim, J. Moon, S. Hong and J. Yi, *J. Membr. Sci.*, 2007, **301**, 118.
25 K. Lam, K. Yeung and G. Nckay, *Environ. Sci. Technol.*, 2007, **41**, 3329.
26 HMAS was immersed in 1.0 M iron nitrate solution for 24 h instead of the vacuum nano-casting route and with other treatments the same, here, C-HMAS was also calcined at 773 K for 2 h as a reference.
27 M. Ohmori and E. Matijevic, *J. Colloid Interface Sci.*, 1993, **160**, 288.
28 S. Ross, *Inorganic Infrared and Raman Spectra*, McGraw-Hill, London, 1972.

